A minimalistic computational model of nucleocytoplasmic transport[*]

Abstract. We develop a minimalistic computational model of nucleocytoplasmic transport that mimics the live cell and (more closely) a hypothetical artificial cell. We are particularly interested in the nuclear-to-cytoplasmic contrast of certain molecular species at steady state, namely, RanGTP, transport receptors, and cargo, since these can be measured in experiments.

Abbreviations. NCT = nucleocytoplasmic transport; NPC = nuclear pore complex; NE = nuclear envelope; IBB = importin beta binding; ODE = ordinary differential equations; FG-nups = FG-nucleoporins; SPR = surface plasmon resonance; N:C = nuclear-to-cytoplasmic.

1 Introduction

The base layer of NCT is the RanGTP gradient for which we use the "minimal Ran gradient system" of [GSR03]; see §2.1. Still following [GSR03], we add importin-mediated transport for IBB cargos. i.e. cargos that do not require an adapter. In this model, the nuclear pore is chemically inert and only serves as a diffusion channel, but in the cell this is not the case. To model that, we first abstract the base layer into a single Ran gradient pump characterized by a single rate, Eqn. 1.

In §2.2 we take a look at the role of RanBP1 in the hydrolysis of RanGTP and associated species but for simplicity abstract this process into one hydrolysis rate, Eqn. (9).

Finally, in §2.3 we develop a computational model that focuses on the main players of NCT, that is, RanGTP, Impβ (karyopherin-beta), Impα (karyopherin-alpha), CAS (exportin), NLS (cargo) and the nuclear pore itself. In this model, any species transits the NPC in these steps: binding to one side of the pore, passing into the pore channel, binding to the other side, and unbinding on the other side. This allows us to reproduce the accumulation of transport receptors inside the NPC.

Each computational model is formulated as an ODE in MATLAB/SimBiology. In addition to kinetic parameters this requires the initial concentrations of all chemical species. We

---

2022-05-09 07:28:26+02:00

compute the ODE numerically until steady state and report the final concentrations in nucleus, cytoplasm and at the nuclear envelope, where applicable.

2 NCT models

2.1 GSR'03 model of NCT

Ran gradient. The Ran gradient, i.e. the nuclear accumulation of RanGTP, is the base layer of nucleocytoplasmic transport. We implement it as the "minimal Ran gradient system" from [GSR03, Fig. 1, Fig. 2, etc.]. The equations are recapitulated in §3 and the constants are collected in Table 2. This gradient can be harnessed by converting nuclear RanGTP back to cytoplasmic RanGDP. For this reason, [GSR03] introduced the "dynamic capacity" Ex as the maximal possible steady-state (positive) flux of nuclear RanGTP to cytoplasmic RanGDP. We determine it using the additional equation (17).

The fluxes are in units of concentration per time (µM/s). The ones across the nuclear boundary have positive sign when exiting the nucleus and are normalized to the nuclear volume. Thus, the *amount* exiting the nucleus per unit of time is $\mathsf{flux} \times V_{\mathrm{nuc}}$.

Simulating the ODE across the scenarios of [GSR03] we obtain results that are sufficiently close to the original, see Table 3. Importantly, an order of 1000x nuclear enrichment of RanGTP is sustained in steady-state. Moreover, the dynamic capacity clocks in at around $0.6\,\mu\mathrm{M/s}$ in most cases, meaning the Ran gradient is established within seconds. Therefore, we will replace the whole Ran gradient layer by a virtual pump

$$\text{cytoplasmic RanGDP} \longrightarrow \text{nuclear RanGTP} \quad \text{with kinetic rate } 0.1\,\mathrm{s}^{-1}. \tag{1}$$

This rate is chosen conservatively (a concentration of $1\,\mu\mathrm{M}$ of cytoplasmic RanGDP generates a flux of $0.1\,\mu\mathrm{M/s}$) but it will be sufficient for our purposes. See Code #1.

Coupling of importin-mediated transport. A coupling of the Ran gradient to importin–cargo transport was proposed in [GSR03, Fig. 6A]. This model thus includes kinetics of Impβ and IBB cargo, in addition to the Ran gradient. Few details were provided in [GSR03], so we formulate a version of it here explicitly. An important omission in this model is the reaction of $\mathsf{Imp\beta \cdot Ran \cdot GTP}$ with $\mathsf{RanBP1}$, which facilitates hydrolysis; on the other hand, the inhibition of hydrolysis by Impβ is absent, as well, cf. the discussion in §2.2. The following equations comprise the handling of cargo by Impβ in the cytoplasm,

$$\tfrac{\mathrm{d}}{\mathrm{d}t}[\mathsf{Imp\beta \cdot Ran \cdot GTP}]_{\mathsf{cyt}} = -\mathsf{R_{cyt}} + \mathsf{F_{Imp\beta \cdot Ran \cdot GTP}}\tfrac{V_{\mathrm{nuc}}}{V_{\mathrm{cyt}}} - \mathsf{GAP_{Imp\beta}} + \mathsf{Knockoff_{cyt}} \tag{2a}$$

$$\tfrac{\mathrm{d}}{\mathrm{d}t}[\mathsf{Imp\beta}]_{\mathsf{cyt}} = +\mathsf{R_{cyt}} + \mathsf{C_{cyt}} + \mathsf{F_{Imp\beta}}\tfrac{V_{\mathrm{nuc}}}{V_{\mathrm{cyt}}} + \mathsf{GAP_{Imp\beta}} \tag{2b}$$

$$\tfrac{\mathrm{d}}{\mathrm{d}t}[\mathsf{Imp\beta \cdot Cargo}]_{\mathsf{cyt}} = -\mathsf{C_{cyt}} + \mathsf{F_{Imp\beta \cdot Cargo}}\tfrac{V_{\mathrm{nuc}}}{V_{\mathrm{cyt}}} - \mathsf{Knockoff_{cyt}} \tag{2c}$$

$$\tfrac{\mathrm{d}}{\mathrm{d}t}[\mathsf{Cargo}]_{\mathsf{cyt}} = +\mathsf{C_{cyt}} + \mathsf{F_{Cargo}}\tfrac{V_{\mathrm{nuc}}}{V_{\mathrm{cyt}}} + \mathsf{Knockoff_{cyt}} \tag{2d}$$

with the fluxes

$$R_{\mathsf{cyt}} := -k_{\mathrm{on}}^{\mathrm{R}}[\mathsf{Imp\beta}][\mathsf{Ran \cdot GTP}]_{\mathrm{cyt}} + k_{\mathrm{off}}^{\mathrm{R}}[\mathsf{Imp\beta \cdot Ran \cdot GTP}]_{\mathrm{cyt}} \tag{3a}$$

$$C_{\mathsf{cyt}} := -k_{\mathrm{on}}^{\mathrm{C}}[\mathsf{Imp\beta}][\mathsf{Cargo}]_{\mathrm{cyt}} + k_{\mathrm{off}}^{\mathrm{C}}[\mathsf{Imp\beta \cdot Cargo}]_{\mathrm{cyt}}. \tag{3b}$$

The forward flux of the reaction

$$\mathsf{Imp\beta \cdot Cargo + Ran \cdot GTP} \; \rightleftharpoons \; \mathsf{Imp\beta \cdot Ran \cdot GTP + Cargo} \tag{4}$$

is called Knockoff. It is modeled as a one-way reaction with forward rate k_{knockoff}. The equations of [GSR03] are modified accordingly:

$$\tfrac{\mathrm{d}}{\mathrm{d}t}[\mathsf{Ran \cdot GDP}]_{\mathrm{cyt}} = (11\mathrm{a}) + \mathsf{GAP}_{\mathsf{Imp\beta}} \tag{11a$'$}$$

$$\tfrac{\mathrm{d}}{\mathrm{d}t}[\mathsf{Ran \cdot GTP}]_{\mathrm{cyt}} = (11\mathrm{b}) + R_{\mathsf{cyt}} - \mathsf{Knockoff}_{\mathsf{cyt}} \tag{11b$'$}$$

Analogous nuclear equations (without GAP) are implemented, but are omitted here. Analogously to (15a)/(15b) we have the additional nuclear-to-cytoplasmic diffusion fluxes
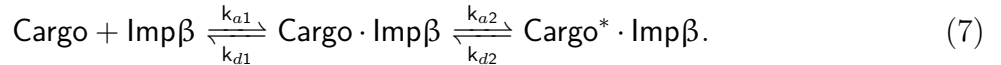
$$F_{\mathsf{Imp\beta \cdot Ran \cdot GTP}}, \quad F_{\mathsf{Imp\beta}}, \quad F_{\mathsf{Imp\beta \cdot Cargo}}, \quad F_{\mathsf{Cargo}} \tag{5}$$

with the permeability constants given in Table 1.

SPR experiments of [Cat+01] indicated that the IBB domain of importin-α binds importin-β and undergoes a conformational change,

$$\mathsf{A + B} \rightleftharpoons \mathsf{AB} \rightleftharpoons \mathsf{A^*B}. \tag{6}$$

We therefore assume the analogous reaction

$$\mathsf{Cargo + Imp\beta} \; \underset{k_{d1}}{\overset{k_{a1}}{\rightleftharpoons}} \; \mathsf{Cargo \cdot Imp\beta} \; \underset{k_{d2}}{\overset{k_{a2}}{\rightleftharpoons}} \; \mathsf{Cargo^* \cdot Imp\beta}. \tag{7}$$

Examples of the kinetic constants are available in [Cat+01, Table I], e.g.,

$$k_{a1} = 0.11\,\mathrm{\mu M^{-1}\,s^{-1}}, \quad k_{d1} = 0.024\,\mathrm{s^{-1}}, \qquad k_{a2} = 0.024\,\mathrm{s^{-1}}, \quad k_{d2} = 7.4 \times 10^{-4}\,\mathrm{s^{-1}}, \tag{8}$$

for an IBB domain binding to Impβ. The intermediate state in (6) is transient on a moderately relevant time-scale (Code #2). Therefore, here we lump the complexed states together and take $k_{\mathrm{on}}^{\mathrm{C}} := k_{a1}$ and $k_{\mathrm{off}}^{\mathrm{C}} := k_{d1}\frac{k_{d2}}{k_{a2}+k_{d2}}$ as the effective kinetic rates for (3b), cf. Table 1.

With the constants from Table 1, the steady-state of the model (reached after some 10^4 s) is reported in Fig. 1. Nuclear accumulation of free cargo is 37-fold. Sensitivity analysis shows that, in relative terms, the final nuclear concentration of free cargo depends most strongly on k_{knockoff}. Doubling k_{knockoff} almost doubles the nuclear concentration. See Code #3.

This model predicts a slight accumulation of Imgβ in the nucleus, with $\mathsf{Imp\beta \cdot Ran \cdot GTP}$ contributing most of the excess.
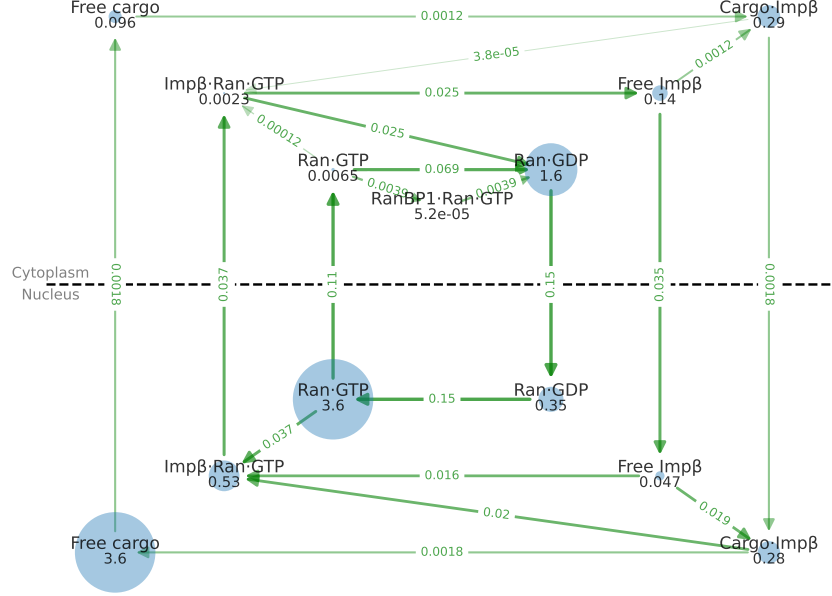
Figure 1: Steady-state of the transport system from §2.1 with conditions of Table 1. The free cargo shows 37-fold accumulation in the nucleus; total nuclear to total cytoplasmic cargo is 10-fold. Units are µM for species and $\mu\text{M s}^{-1}$ for fluxes. Initial conditions: $[\text{Ran} \cdot \text{GDP}]_{\text{cyt}} = 5\,\mu\text{M}$, $[\text{Imp}\beta]_{\text{cyt}} = 1\,\mu\text{M}$, $[\text{Cargo}]_{\text{cyt}} = 3\,\mu\text{M}$, all else zero.

(3a)	$k_{\text{on}}^{\text{R}} = 0.096\,\mu\text{M}^{-1}\,\text{s}^{-1}, \quad k_{\text{off}}^{\text{R}} = 4.8 \times 10^{-6}\,\text{s}^{-1}$	[GSR03, Supp. Table A], [RM05, Table II]
(3b)	$k_{\text{on}}^{\text{C}} = 0.11\,\mu\text{M}^{-1}\,\text{s}^{-1}, \quad k_{\text{off}}^{\text{C}} = 7.2 \times 10^{-4}\,\text{s}^{-1}$	[Cat+01, Table I], [RM05, Table II]
(4)	$k_{\text{knockoff}} = 2 \times 10^{-2}\,\mu\text{M}^{-1}\text{s}^{-1}$	[RM05, Table II]
(5)	$D_{\text{Imp}\beta \cdot \text{Ran} \cdot \text{GTP}} = 0.07\,\text{s}^{-1}, \quad D_{\text{Imp}\beta} = 0.4\,\text{s}^{-1}$ $D_{\text{Imp}\beta \cdot \text{Cargo}} = 0.25\,\text{s}^{-1}, \quad D_{\text{Cargo}} = 5 \times 10^{-4}\,\text{s}^{-1}$	[RM05, Table III]

Table 1: Constants for the Impβ-mediated transport from §2.1.

2.2 GTP hydrolysis and role of RanBP1

According to [LM97, Fig. 4A], Impβ blocks hydrolysis of RanGTP by RanGAP but RanBP1 rescues it for most part. Similarly, [BG97] showed that RanBP1 transiently detaches Ran from the complex Kap · RanGTP (where Kap is some karyopherin), whereupon hydrolysis by RanGAP disassembles the complex; and that efficient disassembly of Impβ · RanGTP required RanBP1 *and* Impα [BG97, §3.2, cf. Fig. 4], [FBR97]. Notably, Kaps and RanBP1 bind Ran at distinct sites [BG97, p.253].

Further, [See+03, Fig. 13] characterizes the kinetics of the formation of the complex between RanGTP, RanBP1 and RanGAP and the GTP hydrolysis. In particular, the release rate of the γ-phosphate, on the order or $10\,\mathrm{s}^{-1}$ in [See+03, Fig. 13], is barely influenced by RanBP1, which instead stimulates the association of Ran with RanGAP. A computational model of hydrolysis with these parameters qualitatively reproduces the experimental data from [LM97, Fig. 4A]. We omit the details that can be found in Code #4.

For simplicity, we will take the constant

$$\text{GTP hydrolysis rate of } 0.1\,\mathrm{s}^{-1} \tag{9}$$

for all cytoplasmic-side species containing RanGTP, and no GTP hydrolysis elsewhere. This should be compared with the effective Ran gradient rate (1). Reducing this rate even 1000-fold does not substantially change the subsequent results (not shown).

2.3 NPC as compartment

Introduction. It has been observed, see [KKL21] and references therein, that Impβ accumulates inside the NPCs as they bind to the FG-nups ("rim staining"), suggesting a regulatory role, and possibly shuttling the cargo across the pore repeatedly. To account for this we propose a model with cytoplasm, nucleus and the NPCs as three compartments. The following dual observation is essential, cf. [Hof20, §10]:

1. cytoplasmic and nuclear species initially react with NPC components in proportion to the number of NPCs, and

2. the observed fluorescence signal from Kaps accumulating inside the NPCs scales with the total volume or the capacity of the NPC channel (rather than their number).

The model includes the following main components:

- Impβ (a.k.a. Kapβ1) and the cargo adapter Impα (a.k.a. Kapα). For simplicity, we do not model individual variants/paralogs/isoforms, cf. [KKL21, p. 2].

- Generic NLS cargo, by itself unable to transition the nuclear envelope efficiently. Requires the Impα adapter in order to be captured by Impβ.

- CAS (a.k.a. Exp2, Xpo2). Recycles Impα back to the cytoplasm.

- The NPCs are described as vacant NPC channel space, the cytoplasm-facing opening NPC(c) and the nucleus-facing opening NPC(n). To transition the nuclear pore, a species has to bind to the opening, transition into the channel, bind to the other opening, and unbind on the other side. This allows us to model the capacity of the NPC and the dwelling time (but we make no distinction between different transiting species). There is no directionality, i.e. a species currently residing in the channel is equally likely to bind to either opening next.

- Ran $\cdot$ GTP in the nucleus and Ran $\cdot$ GDP in the cytoplasm. The consumption of Ran $\cdot$ GTP that have transitioned to the cytoplasmic side by hydrolysis is compensated by an effective pump as in Eqn. (1). The hydrolysis itself is described by one effective kinetic rate as in Eqn. (9).

An overview of the model is shown in Fig. 2. The code is found in Code #5. The computational results for this model are summarized in Fig. 3/4. For details visit the URL

$$\text{https://numpde.github.io/nct1/code/20211018-Appli/checkpoint/20220508-082816/} \qquad (10)$$

Main reactions. Here we comment on the main reactions of the model. For the complete set we refer to Fig. 2 as well as the URL (10).

- The nuclear Ran $\cdot$ GTP is converted directly to cytoplasmic Ran $\cdot$ GDP as in Eqn. (1).

- The Impβ can shuttle on its own through the NPC or in complex with Impα. We assume that the complex does not form on the nuclear side (due to nuclear Ran $\cdot$ GEF, which is not modeled explicitly).

- The cytoplasmic NLS cargo associates with free cytoplasmic Impα $\cdot$ Impβ before binding to the cytoplasmic side of the NPC, or with those already attached there. Once the complex is shuttled to the nuclear side, the "knockoff" reaction releases the cargo (the suffix (n) is omitted):

    Ran $\cdot$ GTP + NLS $\cdot$ Impα $\cdot$ Impβ $\cdot$ NPC $\longrightarrow$ Ran $\cdot$ GTP $\cdot$ Impβ $\cdot$ NPC + Impα + NLS.
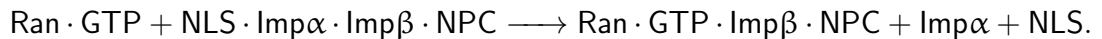
    Thereupon, the complex Ran $\cdot$ GTP $\cdot$ Impβ can transition from the nuclear to the cytoplasmic side to be hydrolized as in Eqn. (9).

- Like Impβ, CAS can shuttle through the NPC. On the nuclear side, it first binds to Ran $\cdot$ GTP then forms the Impα $\cdot$ CAS $\cdot$ Ran $\cdot$ GTP complex, which can shuttle through the NPC, and is disassembled on the cytoplasmic side by the hydrolysis reaction (9).

Baseline parameters. Here we comment on the choice of selected model parameters, such as concentrations and kinetic rates. For the complete set see the URL (10).

- The nucleus and the cytoplasm each have a volume of 1 pL.

- We estimate the total NPC channel capacity as 2000 NPCs per nuclear envelope [BioNumbers, #111130] times 300 Kaps per NPC [Par+07, Fig. 7]. Note that $1\,\mu M \times 1\,pL \approx 300 \times 2000$ units, which implies a concentration of $1\,\mu M$ in a computational volume of $1\,pL$. The computation itself is performed in amounts (not concentration), so to convert to apparent concentration of Kaps at the NE we estimate the volume of the NE as $0.01\,pL$. This only scales the concentrations shown in the figures.

- For the initial concentration of Impβ we take $5\,\mu M$ in nucleus and cytoplasm based on [KKL21, Fig. 4] / [NPW19, Fig. 4a].

- For the initial concentration of Impα we considered $5\,\mu M$ throughout the cell based on the immunoblots of [ZAH13, Fig. 7] and the mass spectrometry measurements for KPNAs from [Wüh+14, Table S5]. This corresponds to all variants of Kapα (KPNA2,3,4,6). However, this seemed incompatible with other parameters, e.g. the NLS remained tied to Impα and nearly equal at nuclear and cytoplasmic sides. We settled on the Impα concentration of $0.5\,\mu M$ for the baseline model, which is close to the previously reported concentration of the single Kapα1 (KPNA2).

Simulating this scenario we observe

- strong accumulation of NLS cargo in the nucleus, most of it free;

- no N:C contrast for Impβ, with some accumulation at the nuclear envelope;

- a N:C contrast of 3:1 for Impα, almost all of it bound;

- a N:C contrast of about 1:4 for free CAS and 4:3 for all CAS;

- about 70% of initial Ran·GTP unbound in the nucleus.

Variants. We define a handful of scenarios to illustrate how parameter choice affects the steady-states. These changes could mimic different cell types, disease or configurations of the artificial cell. They can be generated in vivo by depletion (e.g. via siRNA) or by transfection with a vector overexpressing a protein. The results are summarized in Fig. 3/4. All parameter changes are with respected to the baseline scenario, and are documented in full at the URL (10). We expect the artificial cell to reproduce those trends.

1. Decrease Impβ 10x. We observe a higher N:C contrast of cargo and of Impα.

2. Increase the number of NPCs 10x. More transport receptors are now bound to the NPC, thus exhibiting a higher concentration at the nuclear envelope, cf. [Kal+22].

3. Increase Impα 10x. We observe a breakdown of transport.

4. Decrease Impα 10x. Leads to enhanced N:C contrasts of CAS, Impα and NLS cargo.

5. Turn off Ran·GTP regeneration, starting from the baseline scenario. We obtain a breakdown of N:C contrast for all species, as expected.
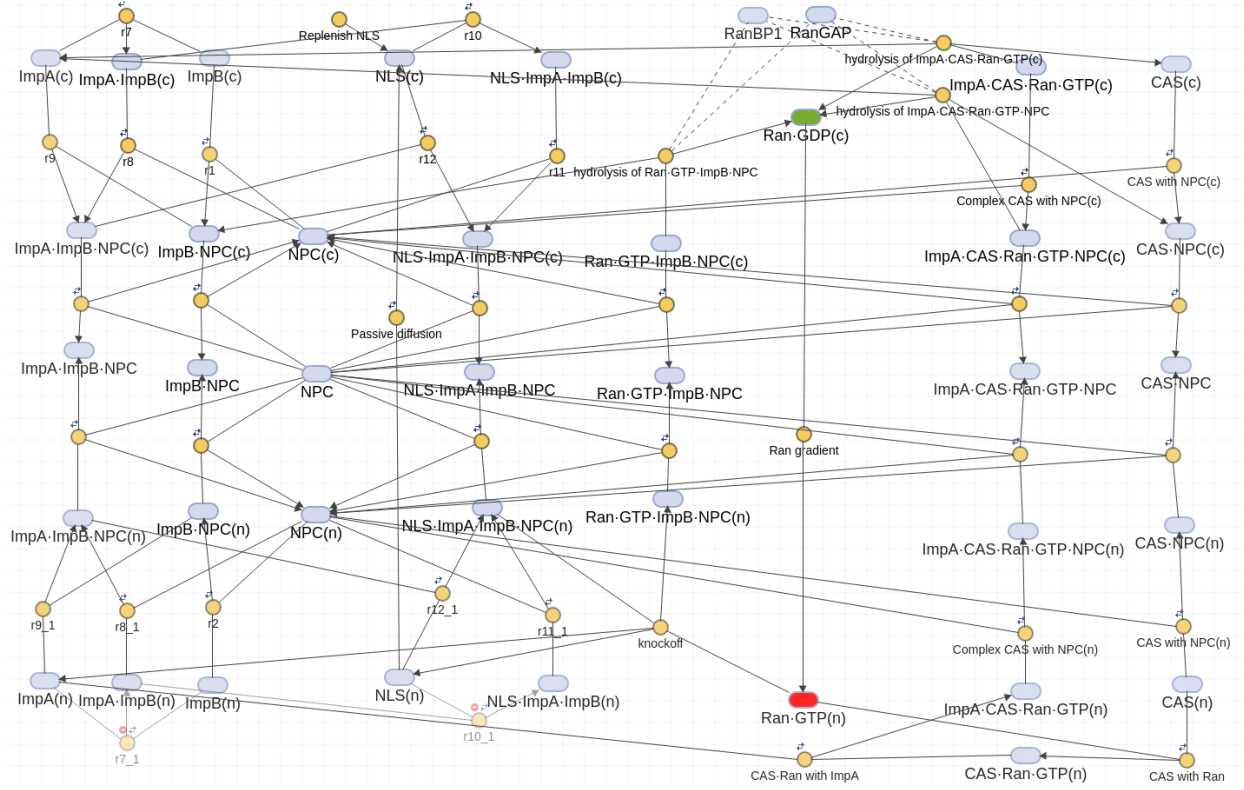
Figure 2: SimBiology diagram for the model "NPC as compartment" from §2.3. The ovals represent chemical species, the yellow circles are reactions (some are reversible). The middle row (containing free NPC) are species inside the NPC. The row above and below are species bound to the cytoplasmic-side and nuclear-side of the NPCs, respectively. The top row are cytoplasmic species and the bottom row are nuclear species. Details at URL (10).
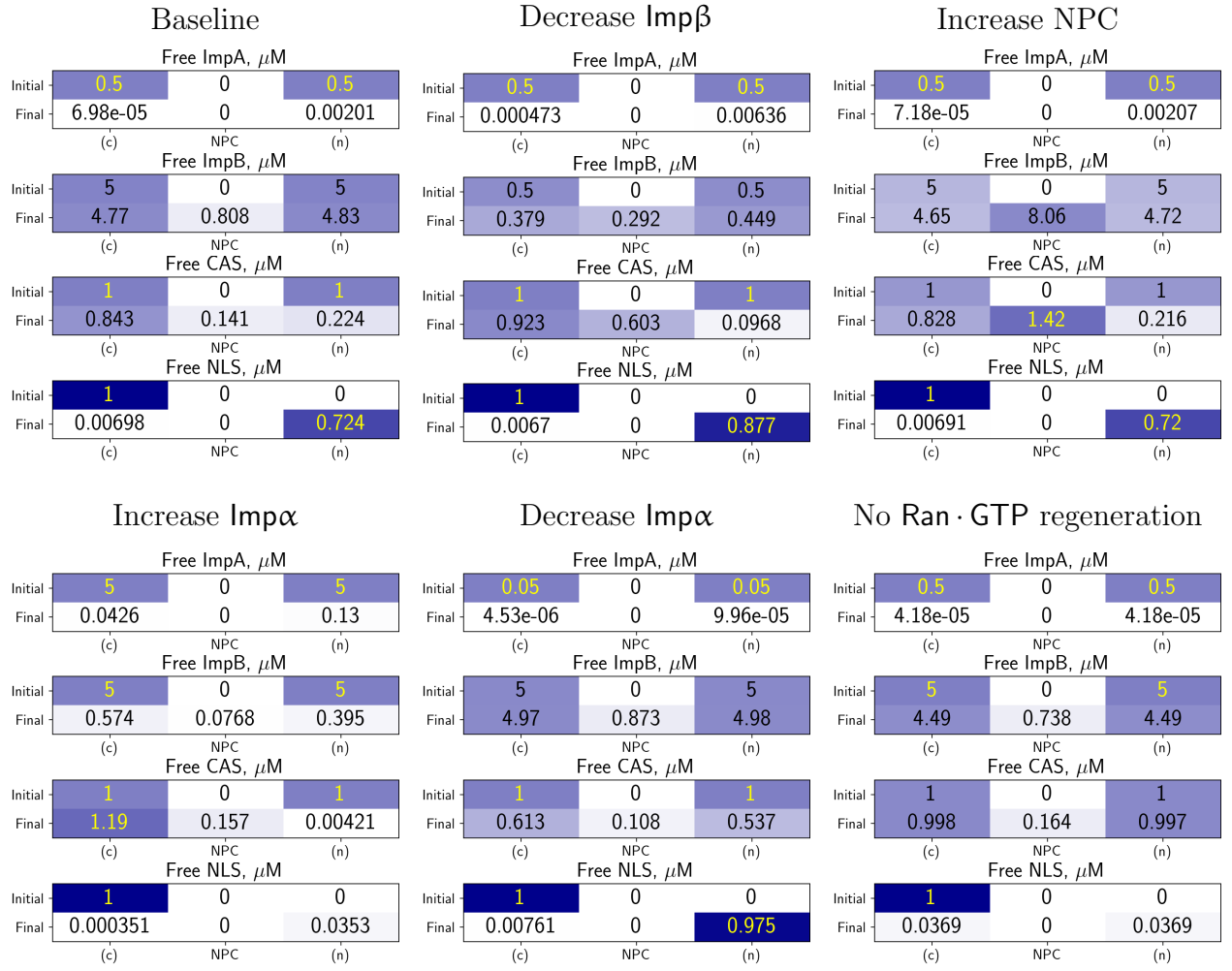
Baseline

Free ImpA, μM

	(c)	NPC	(n)
Initial	0.5	0	0.5
Final	6.98e-05	0	0.00201

Free ImpB, μM

	(c)	NPC	(n)
Initial	5	0	5
Final	4.77	0.808	4.83

Free CAS, μM

	(c)	NPC	(n)
Initial	1	0	1
Final	0.843	0.141	0.224

Free NLS, μM

	(c)	NPC	(n)
Initial	1	0	0
Final	0.00698	0	0.724

Decrease Impβ

Free ImpA, μM

	(c)	NPC	(n)
Initial	0.5	0	0.5
Final	0.000473	0	0.00636

Free ImpB, μM

	(c)	NPC	(n)
Initial	0.5	0	0.5
Final	0.379	0.292	0.449

Free CAS, μM

	(c)	NPC	(n)
Initial	1	0	1
Final	0.923	0.603	0.0968

Free NLS, μM

	(c)	NPC	(n)
Initial	1	0	0
Final	0.0067	0	0.877

Increase NPC

Free ImpA, μM

	(c)	NPC	(n)
Initial	0.5	0	0.5
Final	7.18e-05	0	0.00207

Free ImpB, μM

	(c)	NPC	(n)
Initial	5	0	5
Final	4.65	8.06	4.72

Free CAS, μM

	(c)	NPC	(n)
Initial	1	0	1
Final	0.828	1.42	0.216

Free NLS, μM

	(c)	NPC	(n)
Initial	1	0	0
Final	0.00691	0	0.72

Increase Impα

Free ImpA, μM

	(c)	NPC	(n)
Initial	5	0	5
Final	0.0426	0	0.13

Free ImpB, μM

	(c)	NPC	(n)
Initial	5	0	5
Final	0.574	0.0768	0.395

Free CAS, μM

	(c)	NPC	(n)
Initial	1	0	1
Final	1.19	0.157	0.00421

Free NLS, μM

	(c)	NPC	(n)
Initial	1	0	0
Final	0.000351	0	0.0353

Decrease Impα

Free ImpA, μM

	(c)	NPC	(n)
Initial	0.05	0	0.05
Final	4.53e-06	0	9.96e-05

Free ImpB, μM

	(c)	NPC	(n)
Initial	5	0	5
Final	4.97	0.873	4.98

Free CAS, μM

	(c)	NPC	(n)
Initial	1	0	1
Final	0.613	0.108	0.537

Free NLS, μM

	(c)	NPC	(n)
Initial	1	0	0
Final	0.00761	0	0.975

No Ran·GTP regeneration

Free ImpA, μM

	(c)	NPC	(n)
Initial	0.5	0	0.5
Final	4.18e-05	0	4.18e-05

Free ImpB, μM

	(c)	NPC	(n)
Initial	5	0	5
Final	4.49	0.738	4.49

Free CAS, μM

	(c)	NPC	(n)
Initial	1	0	1
Final	0.998	0.164	0.997

Free NLS, μM

	(c)	NPC	(n)
Initial	1	0	0
Final	0.0369	0	0.0369

Figure 3: Initial states and final steady-states for the model "NPC as compartment" from §2.3 at the cytoplasmic side (c), inside the NPCs (NPC) and at the nuclear side (n), for **free ImpA**, **free ImpB**, **free CAS** and **free NLS cargo**. For full-size figures and time-course plots, see the URL (10).
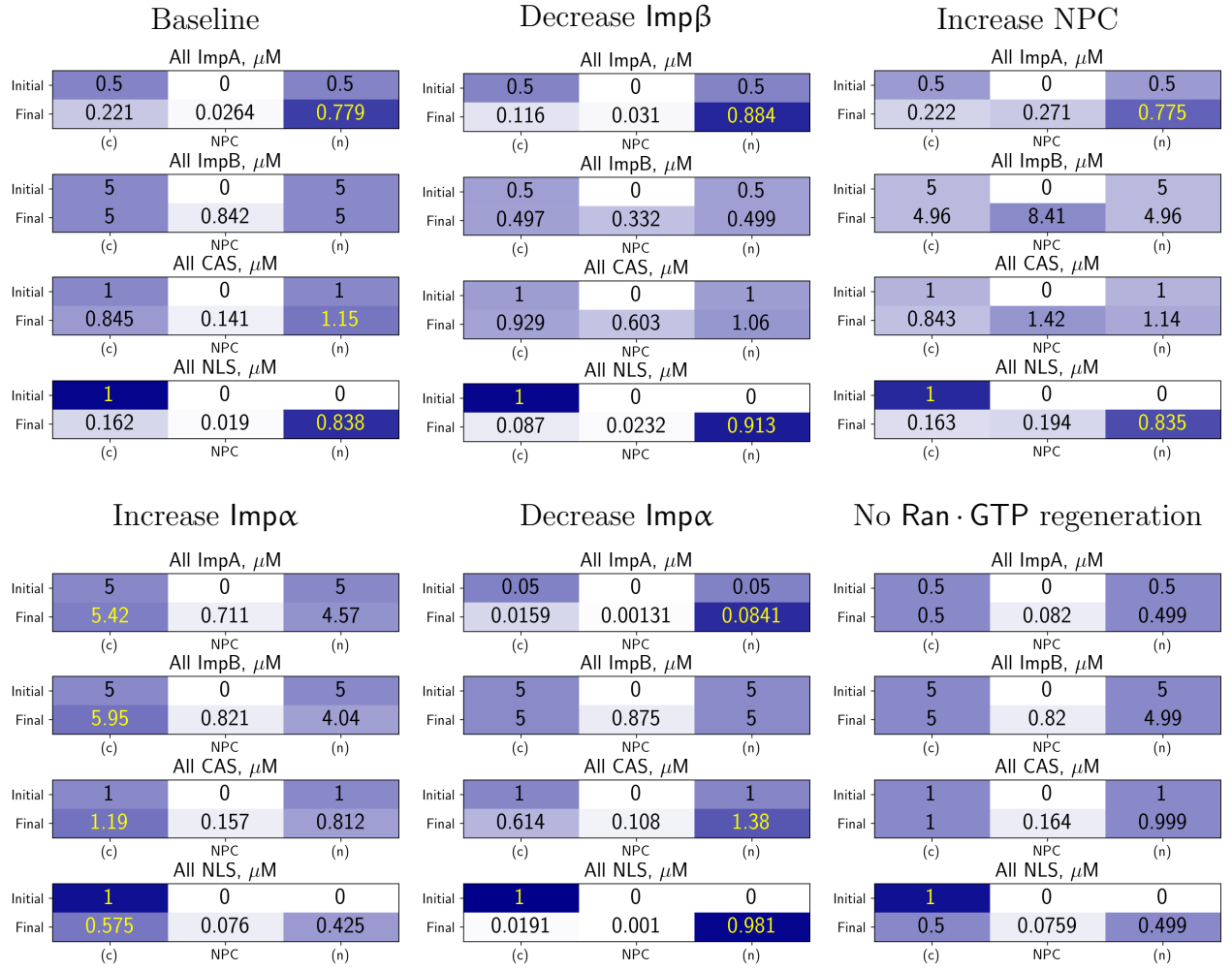
Baseline

All ImpA, μM

	(c)	NPC	(n)
Initial	0.5	0	0.5
Final	0.221	0.0264	0.779

All ImpB, μM

	(c)	NPC	(n)
Initial	5	0	5
Final	5	0.842	5

All CAS, μM

	(c)	NPC	(n)
Initial	1	0	1
Final	0.845	0.141	1.15

All NLS, μM

	(c)	NPC	(n)
Initial	1	0	0
Final	0.162	0.019	0.838

Decrease Impβ

All ImpA, μM

	(c)	NPC	(n)
Initial	0.5	0	0.5
Final	0.116	0.031	0.884

All ImpB, μM

	(c)	NPC	(n)
Initial	0.5	0	0.5
Final	0.497	0.332	0.499

All CAS, μM

	(c)	NPC	(n)
Initial	1	0	1
Final	0.929	0.603	1.06

All NLS, μM

	(c)	NPC	(n)
Initial	1	0	0
Final	0.087	0.0232	0.913

Increase NPC

All ImpA, μM

	(c)	NPC	(n)
Initial	0.5	0	0.5
Final	0.222	0.271	0.775

All ImpB, μM

	(c)	NPC	(n)
Initial	5	0	5
Final	4.96	8.41	4.96

All CAS, μM

	(c)	NPC	(n)
Initial	1	0	1
Final	0.843	1.42	1.14

All NLS, μM

	(c)	NPC	(n)
Initial	1	0	0
Final	0.163	0.194	0.835

Increase Impα

All ImpA, μM

	(c)	NPC	(n)
Initial	5	0	5
Final	5.42	0.711	4.57

All ImpB, μM

	(c)	NPC	(n)
Initial	5	0	5
Final	5.95	0.821	4.04

All CAS, μM

	(c)	NPC	(n)
Initial	1	0	1
Final	1.19	0.157	0.812

All NLS, μM

	(c)	NPC	(n)
Initial	1	0	0
Final	0.575	0.076	0.425

Decrease Impα

All ImpA, μM

	(c)	NPC	(n)
Initial	0.05	0	0.05
Final	0.0159	0.00131	0.0841

All ImpB, μM

	(c)	NPC	(n)
Initial	5	0	5
Final	5	0.875	5

All CAS, μM

	(c)	NPC	(n)
Initial	1	0	1
Final	0.614	0.108	1.38

All NLS, μM

	(c)	NPC	(n)
Initial	1	0	0
Final	0.0191	0.001	0.981

No Ran·GTP regeneration

All ImpA, μM

	(c)	NPC	(n)
Initial	0.5	0	0.5
Final	0.5	0.082	0.499

All ImpB, μM

	(c)	NPC	(n)
Initial	5	0	5
Final	5	0.82	4.99

All CAS, μM

	(c)	NPC	(n)
Initial	1	0	1
Final	1	0.164	0.999

All NLS, μM

	(c)	NPC	(n)
Initial	1	0	0
Final	0.5	0.0759	0.499

Figure 4: Initial states and final steady-states for the model "NPC as compartment" from §2.3 at the cytoplasmic side (c), inside the NPCs (NPC) and at the nuclear side (n), for **all ImpA**, **all ImpB**, **all CAS** and **all NLS cargo** (as if fluorescently labeled). For full-size figures and time-course plots, see the URL (10).
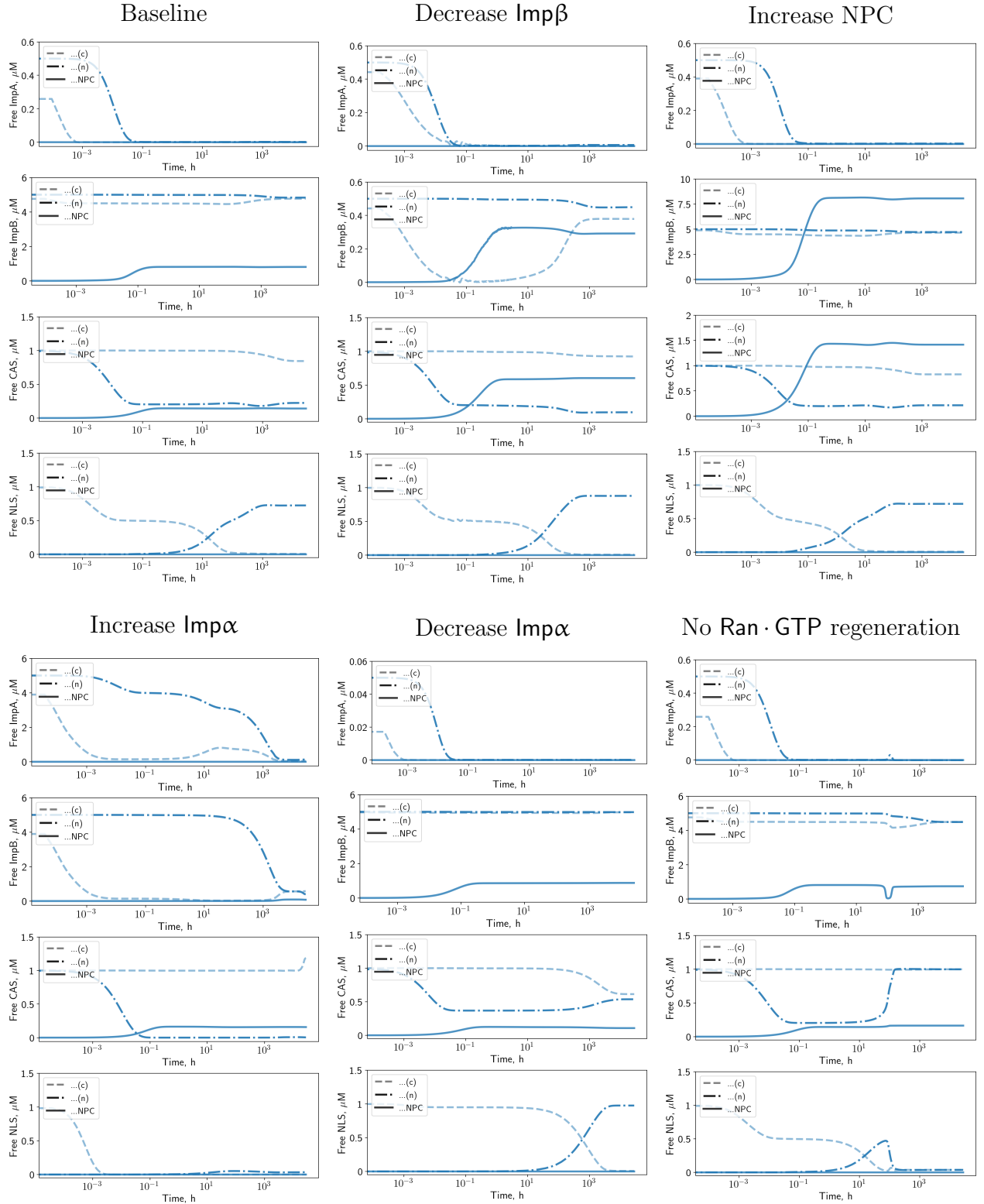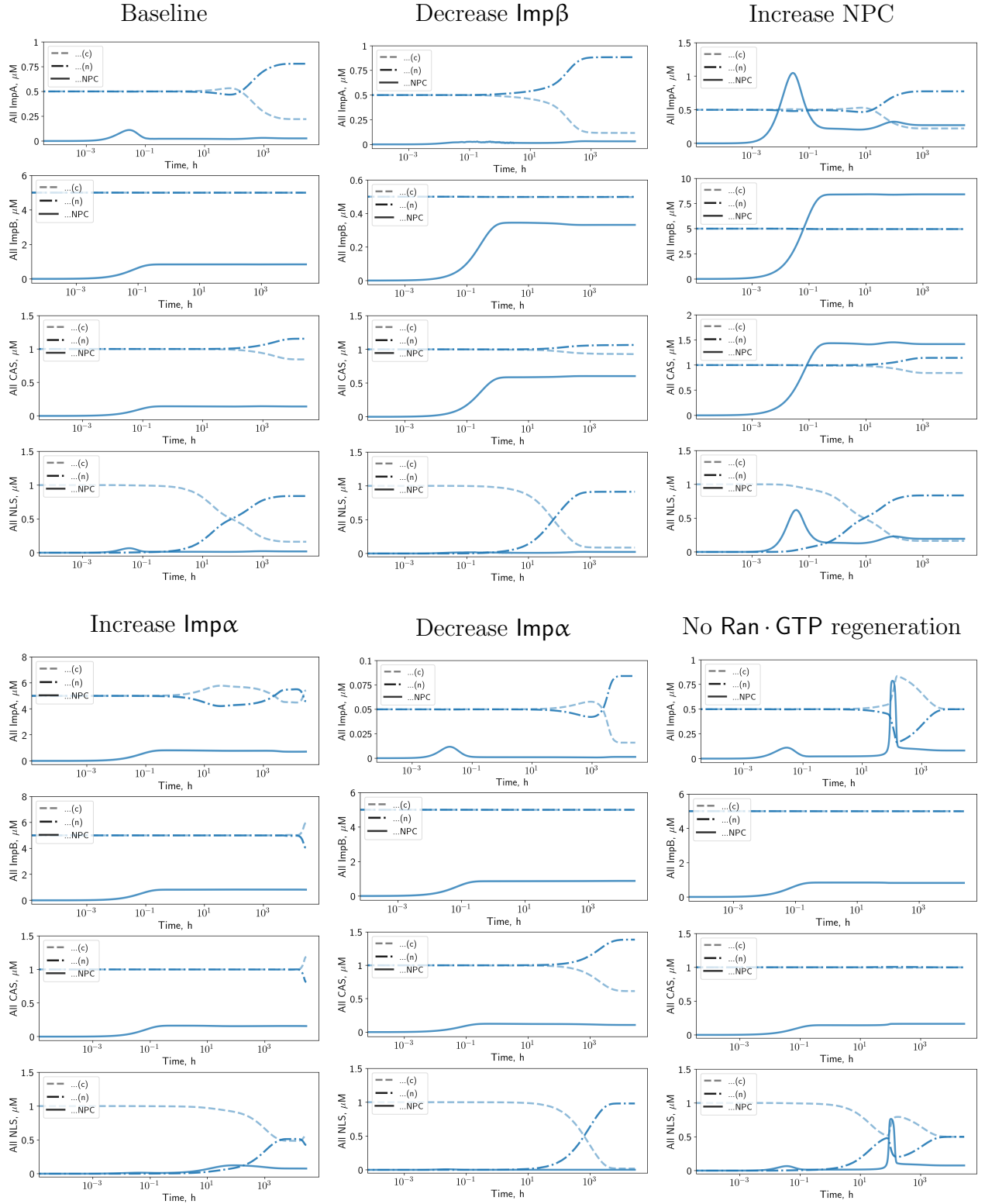
Figure 5: Concentration time-course for the model "NPC as compartment" from §2.3 at the cytoplasmic side (c), inside the NPCs (NPC) and at the nuclear side (n), for **free ImpA**, **free ImpB**, **free CAS** and **free NLS cargo**. For full-size figures and time-course plots, see the URL (10).

11

Figure 6: Concentration time-course for the model "NPC as compartment" from §2.3 at the cytoplasmic side (c), inside the NPCs (NPC) and at the nuclear side (n), for **all ImpA**, **all ImpB**, **all CAS** and **all NLS cargo** (as if fluorescently labeled). For full-size figures and time-course plots, see the URL (10).

12

References

[Bis+95]   F. R. Bischoff, H. Krebber, E. Smirnova, W. Dong, and H. Ponstingl. "Co-activation of RanGTPase and inhibition of GTP dissociation by Ran–GTP binding protein RanBP1". In: *The EMBO Journal* 14.4 (Feb. 1995), pp. 705–715. DOI: 10.1002/j.1460-2075.1995.tb07049.x (cit. on p. 15).

[Kle+95]   C. Klebe, H. Prinz, A. Wittinghofer, and R. S. Goody. "The Kinetic Mechanism of Ran-Nucleotide Exchange Catalyzed by RCC1". In: *Biochemistry* 34.39 (Oct. 1995), pp. 12543–12552. DOI: 10.1021/bi00039a008 (cit. on pp. 15, 16).

[BG97]   F. Bischoff and D. Görlich. "RanBP1 is crucial for the release of RanGTP from importin β-related nuclear transport factors". In: *FEBS Letters* 419.2-3 (Dec. 1997), pp. 249–254. DOI: 10.1016/s0014-5793(97)01467-1 (cit. on p. 5).

[FBR97]   M. Floer, G. Blobel, and M. Rexach. "Disassembly of RanGTP-Karyopherin β Complex, an Intermediate in Nuclear Protein Import". In: *Journal of Biological Chemistry* 272.31 (Aug. 1997), pp. 19538–19546. DOI: 10.1074/jbc.272.31.19538 (cit. on p. 5).

[LM97]   K. M. Lounsbury and I. G. Macara. "Ran-binding Protein 1 (RanBP1) Forms a Ternary Complex with Ran and Karyopherin β and Reduces Ran GTPase-activating Protein (RanGAP) Inhibition by Karyopherin β". In: *Journal of Biological Chemistry* 272.1 (Jan. 1997), pp. 551–555. DOI: 10.1074/jbc.272.1.551 (cit. on p. 5).

[Cat+01]   B. Catimel, T. Teh, M. R. Fontes, I. G. Jennings, D. A. Jans, G. J. Howlett, E. C. Nice, and B. Kobe. "Biophysical Characterization of Interactions Involving Importin-α during Nuclear Import". In: *Journal of Biological Chemistry* 276.36 (Sept. 2001), pp. 34189–34198. DOI: 10.1074/jbc.m103531200 (cit. on pp. 3, 4).

[GSR03]   D. Görlich, M. J. Seewald, and K. Ribbeck. "Characterization of Ran-driven cargo transport and the RanGTPase system by kinetic measurements and computer simulation". In: *The EMBO Journal* 22.5 (Mar. 2003), pp. 1088–1100. DOI: 10.1093/emboj/cdg113 (cit. on pp. 1–4, 15, 16).

[See+03]   M. J. Seewald, A. Kraemer, M. Farkasovsky, C. Körner, A. Wittinghofer, and I. R. Vetter. "Biochemical Characterization of the Ran–RanBP1–RanGAP System: Are RanBP Proteins and the Acidic Tail of RanGAP Required for the Ran-RanGAP GTPase Reaction?" In: *Molecular and Cellular Biology* 23.22 (Nov. 2003), pp. 8124–8136. DOI: 10.1128/mcb.23.22.8124-8136.2003 (cit. on p. 5).

[RM05]   G. Riddick and I. G. Macara. "A systems analysis of importin-α–β mediated nuclear protein import". In: *Journal of Cell Biology* 168.7 (Mar. 2005), pp. 1027–1038. DOI: 10.1083/jcb.200409024 (cit. on p. 4).

[Par+07]   A. Paradise, M. K. Levin, G. Korza, and J. H. Carson. "Significant Proportions of Nuclear Transport Proteins with Reduced Intracellular Mobilities Resolved by Fluorescence Correlation Spectroscopy". In: *Journal of Molecular Biology* 365.1 (Jan. 2007), pp. 50–65. DOI: 10.1016/j.jmb.2006.09.089 (cit. on p. 7).

[ZAH13]   J. Zienkiewicz, A. Armitage, and J. Hawiger. "Targeting Nuclear Import Shuttles, Importins/Karyopherins alpha by a Peptide Mimicking the NFκB1/p50 Nuclear Localization Sequence". In: *JAHA* 2.5 (Sept. 2013). DOI: 10.1161/jaha.113.000386 (cit. on p. 7).

[Wüh+14]   M. Wühr, R. M. Freeman, M. Presler, M. E. Horb, L. Peshkin, S. P. Gygi, and M. W. Kirschner. "Deep Proteomics of the Xenopus laevis Egg using an mRNA-Derived Reference Database". In: *Current Biology* 24.13 (July 2014), pp. 1467–1475. DOI: 10.1016/j.cub.2014.05.044 (cit. on p. 7).

[NPW19]   T. Nguyen, N. Pappireddi, and M. Wühr. "Proteomics of nucleocytoplasmic partitioning". In: *Current Opinion in Chemical Biology* 48 (Feb. 2019), pp. 55–63. DOI: 10.1016/j.cbpa.2018.10.027 (cit. on p. 7).

[Hof20]   J.-H. S. Hofmeyr. "Kinetic modelling of compartmentalised reaction networks". In: 197 (Nov. 2020), p. 104203. DOI: 10.1016/j.biosystems.2020.104203 (cit. on p. 5).

[KKL21]   J. Kalita, L. E. Kapinos, and R. Y. H. Lim. "On the asymmetric partitioning of nucleocytoplasmic transport – recent insights and open questions". In: *Journal of Cell Science* 134.7 (Apr. 2021). DOI: 10.1242/jcs.240382 (cit. on pp. 5, 7).

[Kal+22]   J. Kalita, L. E. Kapinos, T. Zheng, C. Rencurel, A. Zilman, and R. Y. Lim. "Karyopherin enrichment and compensation fortifies the nuclear pore complex against nucleocytoplasmic leakage". In: *Journal of Cell Biology* 221.3 (Jan. 2022). DOI: 10.1083/jcb.202108107 (cit. on p. 7).

List of codes

	page	https://github.com/numpde/nct1/tree/ …
#1	p.2	main/code/20210225-GSR/v1
#2	p.3	main/code/20210407-Rearrangement
#3	p.3	main/code/20210225-GSR/v2
#4	p.5	main/code/20210403-StickyPore/c_rangap-sequence
#5	p.6	main/code/20211018-Appli

'

3 Appendix: minimal Ran gradient system

Here we recapitulate the minimal Ran gradient system from [GSR03, Fig. 2], cf. §2.1. The following account for the cytoplasmic species. Here, [...] abbreviates the (cytoplasmic) concentration of the complex $\mathsf{RanBP1 \cdot Ran \cdot GTP}$. Ex is an additional potentially useful flux of nuclear $\mathsf{Ran \cdot GTP}$ to cytoplasmic $\mathsf{Ran \cdot GDP}$, set by default to zero.

$$\frac{\mathrm{d}}{\mathrm{d}t}[\mathsf{Ran \cdot GDP}]_{\mathrm{cyt}} = \mathsf{F_{Ran \cdot GDP}} \frac{V_{\mathrm{nuc}}}{V_{\mathrm{cyt}}} + \mathsf{GAP} + \mathsf{GAP_{RanBP1}} + \mathsf{Ex}\frac{V_{\mathrm{nuc}}}{V_{\mathrm{cyt}}} \tag{11a}$$

$$\frac{\mathrm{d}}{\mathrm{d}t}[\mathsf{Ran \cdot GTP}]_{\mathrm{cyt}} = \mathsf{F_{Ran \cdot GTP}} \frac{V_{\mathrm{nuc}}}{V_{\mathrm{cyt}}} - \mathsf{GAP} - k_{\mathrm{on}}^{\mathrm{rbp}}[\mathsf{RanBP1}][\mathsf{Ran \cdot GTP}]_{\mathrm{cyt}} + k_{\mathrm{off}}^{\mathrm{rbp}}[\dots] \tag{11b}$$

$$\frac{\mathrm{d}}{\mathrm{d}t}[\mathsf{RanBP1 \cdot Ran \cdot GTP}] = -\mathsf{GAP_{RanBP1}} \quad\quad + k_{\mathrm{on}}^{\mathrm{rbp}}[\mathsf{RanBP1}][\mathsf{Ran \cdot GTP}]_{\mathrm{cyt}} - k_{\mathrm{off}}^{\mathrm{rbp}}[\dots] \tag{11c}$$

The following account for the nuclear species. As in [GSR03], E denotes free $\mathsf{RCC1}$.

$$\frac{\mathrm{d}}{\mathrm{d}t}[\mathsf{Ran \cdot GDP}]_{\mathrm{nuc}} = -\mathsf{F_{Ran \cdot GDP}} + r_8[\mathsf{IntC}] - r_1[\mathsf{E}][\mathsf{Ran \cdot GDP}]_{\mathrm{nuc}} \tag{12a}$$

$$\frac{\mathrm{d}}{\mathrm{d}t}[\mathsf{Ran \cdot GTP}]_{\mathrm{nuc}} = -\mathsf{F_{Ran \cdot GTP}} + r_4[\mathsf{IntA}] - r_5[\mathsf{E}][\mathsf{Ran \cdot GTP}]_{\mathrm{nuc}} - \mathsf{Ex} \tag{12b}$$

The nucleotide-exchange reaction $\mathsf{Ran \cdot GDP + GTP \rightleftharpoons Ran \cdot GTP + GDP}$ is catalyzed by $\mathsf{RCC1}$. It is modeled as in [Kle+95, Fig. 6] / [GSR03, Fig. 1] with three intermediates. Note that it depends on the availability of GDP and GTP.

$$\frac{\mathrm{d}}{\mathrm{d}t}[\mathsf{IntA}] = -(r_4 + r_6)[\mathsf{IntA}] + r_5[\mathsf{E}][\mathsf{Ran \cdot GTP}]_{\mathrm{nuc}} + r_3[\mathsf{GTP}][\mathsf{IntB}] \tag{13a}$$

$$\frac{\mathrm{d}}{\mathrm{d}t}[\mathsf{IntB}] = r_6[\mathsf{IntA}] + r_2[\mathsf{IntC}] - (r_3[\mathsf{GTP}] + r_7[\mathsf{GDP}])[\mathsf{IntB}] \tag{13b}$$

$$\frac{\mathrm{d}}{\mathrm{d}t}[\mathsf{IntC}] = -(r_2 + r_8)[\mathsf{IntC}] + r_1[\mathsf{E}][\mathsf{Ran \cdot GDP}]_{\mathrm{nuc}} + r_7[\mathsf{GDP}][\mathsf{IntB}] \tag{13c}$$

Constraints on the total concentration:

$$\text{Free } \mathsf{RCC1}: \quad\quad [\mathsf{E}] = \mathsf{RCC1}_{\mathrm{total}} - ([\mathsf{IntA}] + [\mathsf{IntB}] + [\mathsf{IntC}]) \tag{14a}$$

$$\text{Free } \mathsf{RanBP1}: \quad\quad [\mathsf{RanBP1}] = \mathsf{RanBP1}_{\mathrm{total}} - [\mathsf{RanBP1 \cdot Ran \cdot GTP}] \tag{14b}$$

Gradient-driven fluxes from the nucleus to the cytoplasm:

$$\mathsf{F_{Ran \cdot GTP}} = D_{\mathsf{Ran \cdot GTP}} ([\mathsf{Ran \cdot GTP}]_{\mathrm{nuc}} - [\mathsf{Ran \cdot GTP}]_{\mathrm{cyt}}) \tag{15a}$$

$$\mathsf{F_{Ran \cdot GDP}} = D_{\mathsf{Ran \cdot GDP}} ([\mathsf{Ran \cdot GDP}]_{\mathrm{nuc}} - [\mathsf{Ran \cdot GDP}]_{\mathrm{cyt}}) \tag{15b}$$

RanGAP hydrolyzes the γ-phosphate of $\mathsf{Ran \cdot GTP}$. This is more efficient when $\mathsf{Ran \cdot GTP}$ is bound to $\mathsf{RanBP1}$ [Bis+95], reducing the IC50 seven-fold [GSR03, Table I, p. 1091].

$$\mathsf{GAP} = k_{\mathsf{GAP}}[\mathsf{RanGAP}]/(1 + K_{\mathsf{GAP}}/[\mathsf{Ran \cdot GTP}]_{\mathrm{cyt}}) \tag{16a}$$

$$\mathsf{GAP_{RanBP1}} = k'_{\mathsf{GAP}}[\mathsf{RanGAP}]/(1 + K'_{\mathsf{GAP}}/[\mathsf{RanBP1 \cdot Ran \cdot GTP}]) \tag{16b}$$

To determine the dynamic capacity Ex at steady-state we introduce the additional equation:

$$\frac{\mathrm{d}}{\mathrm{d}t}\mathsf{Ex} = k_{\mathsf{Ex}}[\mathsf{Ran \cdot GTP}]_{\mathrm{nuc}}, \quad k_{\mathsf{Ex}} := 10\,\mathrm{s}^{-2}, \quad \text{initial} \quad \mathsf{Ex} := 0\,\mu\mathrm{M\,s}^{-1}. \tag{17}$$

(11a)	$V_{\text{nuc}} = 1.2\,\text{pl}, \quad V_{\text{cyt}} = 1.8\,\text{pl}$	[GSR03, Table II]
(11a)	initial condition $[\mathsf{Ran}\cdot\mathsf{GDP}]_{\text{cyt}} = 5\,\mu\text{M}$	[GSR03, Table II]
(11b)–(11c)	$k_{\text{on}}^{\text{rbp}} = 0.3\,\mu\text{M}^{-1}\,\text{s}^{-1}, \quad k_{\text{off}}^{\text{rbp}} = 4\times10^{-4}\,\text{s}^{-1}$	[GSR03, Supp. Table A]
(12a)–(13c)	$r_1 = 74\,\mu\text{M}^{-1}\,\text{s}^{-1}, \quad r_8 = 55\,\text{s}^{-1}$ $r_7 = 11\,\mu\text{M}^{-1}\,\text{s}^{-1}, \quad r_2 = 21\,\text{s}^{-1}$ $r_3 = 0.6\,\mu\text{M}^{-1}\,\text{s}^{-1}, \quad r_6 = 19\,\text{s}^{-1}$ $r_5 = 100\,\mu\text{M}^{-1}\,\text{s}^{-1}, \quad r_4 = 55\,\text{s}^{-1}$	[GSR03, Supp. Table A] [Kle+95, Fig. 6]
(13a)–(13c)	$[\mathsf{GTP}] = 500\,\mu\text{M}, \quad [\mathsf{GDP}] = 1.6\,\mu\text{M}$	[GSR03, Table II]
(14a)	$\mathsf{RCC1}_{\text{total}} = 0.7\,\mu\text{M}$	[GSR03, Supp. Table B]
(14b)	$\mathsf{RanBP1}_{\text{total}} = 2\,\mu\text{M}$	[GSR03, Fig. 4]
(15a)	$D_{\mathsf{Ran}\cdot\mathsf{GTP}} = 0.03\,\text{s}^{-1}$	[GSR03, Table II]
(15b)	$D_{\mathsf{Ran}\cdot\mathsf{GDP}} = 0.12\,\text{s}^{-1}$	
(16a)	$k_{\mathsf{GAP}} = 10.6\,\text{s}^{-1}, \quad K_{\mathsf{GAP}} = 0.7\,\mu\text{M}$	[GSR03, Supp. Table A]
(16b)	$k'_{\mathsf{GAP}} = 10.8\,\text{s}^{-1}, \quad K'_{\mathsf{GAP}} = 0.1\,\mu\text{M}$	[GSR03, Table I]
(16a)–(16b)	cytoplasmic $[\mathsf{RanGAP}] = 0.7\,\mu\text{M}$	[GSR03, Table II / ST B]

Table 2: Constants for the "standard simulation condition" of §2.1 at 25 °C. Except for (11a), all species are initialized to zero at $t = 0$.

Condition	Affected parameters	Nuclear RanGTP, µM	Cytoplasmic RanGTP, nM	Dynamic capacity, µM/s
"Standard"	See Table 2	4.26 (4.3)	7.75 (7.7)	0.59 (0.60)
Omission of RanBP1	$\mathsf{RanBP1}_{\text{total}} := 0$	4.27 (4.3)	8.13 (8.1)	0.59 (0.60)
200% RCC1	$\mathsf{RCC1}_{\text{total}}$	3.95 (4.0)	7.17 (7.1)	0.59 (0.60)
50% RCC1	$\mathsf{RCC1}_{\text{total}}$	4.31 (4.3)	7.82 (7.7)	0.58 (0.60)
10% RCC1	$\mathsf{RCC1}_{\text{total}}$	3.59 (3.6)	6.50 (6.4)	0.46 (0.48)
1% RCC1	$\mathsf{RCC1}_{\text{total}}$	1.40 (1.4)	2.52 (2.5)	0.075 (0.08)
GTP:GDP = 500:0	$[\mathsf{GDP}] := 0\,\mu\text{M}$	4.80 (4.8)	8.72 (8.6)	0.59 (0.60)
GTP:GDP = 500:50	$[\mathsf{GDP}] := \frac{1}{10}[\mathsf{GTP}]$	0.98 (0.8)	1.76 (1.5)	0.57 (0.58)
GTP:GDP = 500:500	$[\mathsf{GDP}] := [\mathsf{GTP}]$	0.12 (0.12)	0.22 (0.21)	0.34 (0.34)
Saturating NTF2	$D_{\mathsf{Ran}\cdot\mathsf{GDP}} := 0.48\,\text{s}^{-1}$	5.12 (5.1)	9.32 (9.2)	2.18 (2.2)
No NTF2	$D_{\mathsf{Ran}\cdot\mathsf{GDP}} := D_{\mathsf{Ran}\cdot\mathsf{GTP}}$	2.55 (2.5)	4.60 (4.5)	0.15 (0.16)
200% RanGAP	$[\mathsf{RanGAP}]$	4.27 (4.3)	3.95 (3.9)	0.59 (0.60)
50% RanGAP	$[\mathsf{RanGAP}]$	4.26 (4.3)	14.9 (14)	0.59 (0.60)
50% permeability	$D_{\mathsf{Ran}\cdot\mathsf{GTP}}$	4.91 (4.9)	4.44 (4.4)	0.59 (–)
200% permeability	$D_{\mathsf{Ran}\cdot\mathsf{GTP}}$	3.41 (3.4)	12.4 (12.3)	0.59 (–)
400% permeability	$D_{\mathsf{Ran}\cdot\mathsf{GTP}}$	2.46 (2.5)	18.0 (17.8)	0.59 (–)

Table 3: Steady-state concentrations for the simulation scenarios from [GSR03, Table II/III], with their results shown in brackets. Value for $D_{\mathsf{Ran}\cdot\mathsf{GDP}}$ is from [GSR03, Fig. 3].